Method for Separation of Coal Conversion Products from Oxygen Carriers

Junior NASAH[1], Ben JENSEN[1], Nicholas DYRSTAD-CINCOTTA[1], Jackson GERBER[1], Daniel LAUDAL[1], Michael MANN[1] and Srivats SRINIVASACHAR[2]

[1] *University of North Dakota – Institute for Energy Studies, 2844 Campus Road, Grand Forks, ND, USA*

[2] *Envergex, LLC, 10 Podunk Road, Sturbridge, MA, USA*

Abstract – Complete fuel conversion represents an important, but unresolved, aspect in Chemical Looping Combustion (CLC). Different system design approaches are currently being investigated to maximize carbon conversion in the fuel reactor. To achieve greater than ninety percent conversion of the fuel in "fluid-bed" type reducers will require that CLC systems be equipped with additional process equipment to ensure that unburnt fuel leaving the reducer is minimized. This paper presents results obtained from a laboratory test system simulating a char stripper design comprising two components; one for separating large char particles, based on material density differentials, and another for removing small char particles from the oxygen carrier (OC) leaving the reducer, based on elutriation. A test unit was designed, built and operated to identify optimum conditions for separating OC material from unburnt solid fuel – char. The results obtained are necessary for designing a high temperature unit operated at temperatures expected within a CLC system.

Keywords – Chemical looping combustion, char stripper, carbon dioxide capture, oxygen carrier.

1 Introduction

Chemical Looping Combustion (CLC) is a promising clean coal technology for producing a near-pure carbon dioxide (CO_2) stream from coal-based power generation. The majority of the CLC technologies worldwide use the configuration of two interconnected bed reactors using an oxygen carrier (OC) that strips oxygen (O_2) from air in one reactor (oxidizer) and delivers it to a fuel reactor (reducer) (Tong et al., 2014; Linderholm and Lyngfelt, 2017; Bayham et al., 2015). In the reducer, the oxygen-rich OC reacts with the fuel to produce a near-pure compression ready CO_2 stream. The OC is then cycled back to the oxidizer to be regenerated. Solid fuels such as coal or biomass are the target fuels for CLC (Mendiara et al., 2018; Azis et al., 2013; Viches et al., 2017). Use of biomass or coal/biomass blends is particularly attractive in CLC as capture and storage of the produced CO_2 would result in 'negative' carbon emissions (Mendiara et al., 2018).

Current CLC development research can be grouped into two categories based on their reducer design: a fluidized bed or a moving bed. The moving bed reducer approach for CLC was pioneered by Ohio State University (Zeng et al., 2012) and consists of a vertical moving bed of OC with coal pneumatically fed to the bed. This approach ensures good contacting between the gas and solid species, with high coal conversions reported (Zeng et al., 2012; Kim et al., 2013). The fluidized bed reactor approach is more common partly due to commercial availability of fluidized bed systems in the Energy and Chemicals industry. It also enables efficient segregation of the solids from the gas streams using cyclones. However, two main problems plague fluidized bed systems when deployed for CLC. The first problem is insufficient time and contacting of combustible gases at temperature to achieve the high conversions needed (Bayham et al., 2015). To resolve this problem, several researchers (Linderholm and Lyngfelt, 2017; Adànez et al., 2018; Sahir, 2013; Abad et al., 2012; Recio et al., 2016; Tian et al., 2015) are focused on developing Chemical Looping Oxygen Uncoupled (CLOU). In this approach, for example, copper oxide (CuO)-based materials are used as the OC, which is purported to release gaseous O_2 in the reducer to combust the fuel. This ensures higher conversion of volatile combustibles.

The second challenge faced by fluidized bed CLC systems is inadequate residence times to ensure complete coal residue (char) conversion (Abad et al., 2011). When a solid fuel such as coal or biomass is used, complete conversion of the fuel is a challenge (Kramp et al., 2012). The capture efficiency of CLC systems hinges on effectively minimizing the amount of fuel that is not converted in the reducer and escapes to the oxidizer. Unconverted solid fuel results in a net penalty on the capture efficiency of the CLC unit. In order to improve fuel conversion in the fuel reactor, several different approaches focusing on equipment design are being explored. For example, researchers have used dual-stage moving beds (Tong et al., 2014; Adànez et al., 2018; Thon et al., 2014), to increase residence time for converting the char. Another method, currently under research by this team (Van Der Watt et al., 2017) involves the use of spouted fluidized beds – a variant of fluidized beds – that improves solid mixing/contacting and residence time of the solid fuel with the oxygen carrier. Additional steps, such as improving the coal reactivity (Gu et al., 2014) and improving mass transfer by using finer coal sizes (Linderholm and Lyngfelt, 2017), have also shown promise, however, too fine a coal could result in higher elutriation of the unconverted solid species to the reducer exhaust. In the absence of an effective solution for minimizing the amount of char exiting the reducer, Kramp et al. (Kramp et al., 2012) and Keairns et al. (Keairns et al., 2014) both recommended that a char "stripper" be installed between the reducer and oxidizer, to segregate the unburnt char material from the OC and to recycle the segregated char to the reducer. This increases the residence time for char conversion in the reducer. Keairns et al. estimated that a minimum of 80 percent of the slip char needed to be recycled to achieve a CO_2 capture rate of about 90 percent (Keairns et al., 2014).

Any char stripper design is required to operate at CLC temperatures of 800-1000°C. At these temperatures and the large physical sizes for full-scale systems, physical processes that rely on density and size differences present the best chance of success. Currently, the types of char strippers in use by other researchers can be summarized as: 1) the paired-cyclone and fluid bed

stripper (Ströhle, Orth and Epple, 2015), 2) the riser-based design to separate the char and OC by their density differences (Abad et al., 2015; Sun et al., 2016; Sun et al., 2015; Johannson, 2016) and 3) increased residence time for char (Markström, Linderholm and Lyngfelt, 2013). This paper presents the work done to develop a Particle Char Segregator (PCS) system for separating char from oxygen carrier (OC) leaving the reducer in a CLC system. The PCS system comprises two complementary processes that separate char from OC based on their difference in minimum fluidization and terminal velocities. The paper focuses on development efforts of the first unit, known as a Large Char Separator (LCS), designed to separate coarse char (greater than approximately 100 µm) from attrited OC, and which has terminal velocities in the same order of magnitude as the char (van der Watt et al., 2017). The second unit is referred to as the Small Char Separator (SCS) which is a riser system similar to existing carbon strippers used with other CLC systems (Johannson, 2016; Abad et al., 2015) and is included as a polishing step for the LCS.

2 Experimental Work

The PCS system comprises two main process units – the Large Char Separator (LCS) and Small Char Separator (SCS). Figure 1 below is schematic of both systems. The LCS system's operating principle is based on differences in minimum fluidization of a two-component fluidized bed (Keller, 2012; Rowe and Nienow, 1976). Solids (for example char) with lower minimum fluidization are segregated to the top of the bed and discharged through the char exit, Figure 1, and denser solids such as oxygen carriers (OC) are discharged through the OC exit. Meanwhile, the SCS operating principle is based on differences in terminal velocity (Kunii and Levenspiel, 1991) – finer particles are elutriated from the top of the bed, while the heavy OC exits through the bottom. Development work presented in this paper focuses first on "proof-of-concept" of the LCS and SCS and then operation as the PCS System.

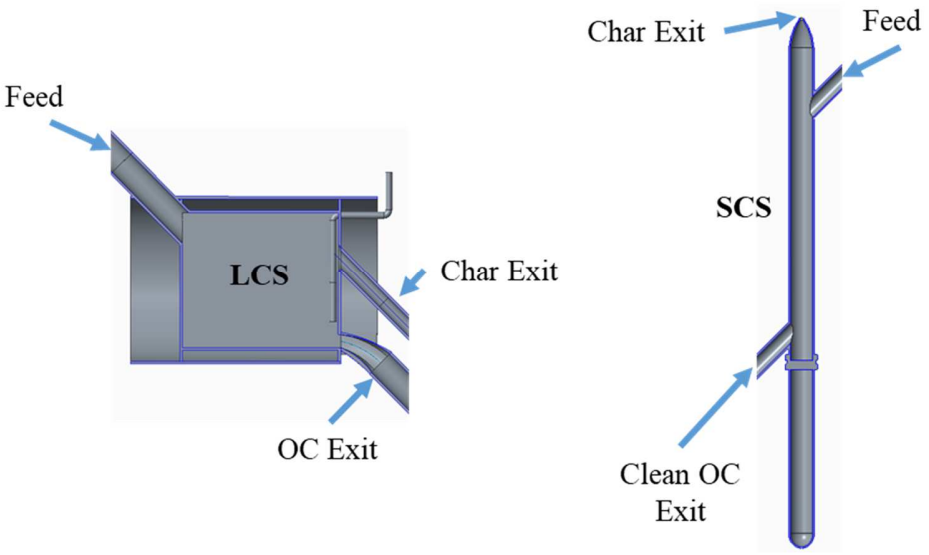

Figure 1. Schematic of LCS (left) and SCS (right) units

2.1 Materials for Proof-of-Concept Testing

Glass beads and activated carbon (AC) were used to simulate the OC and the char respectively. AC was selected as a char substitute due to its similar density with char (~800 kg/m^3) and to avoid reader confusion, we will refer to AC as char throughout the document. The particle size distribution (PSD) used during batch tests is shown in Table 1 below. The density of the glass beads is approximately 2400 kg/m^3. The density of the glass beads is more representative of OC after multiple reduction-oxidation cycles (Cuadrat et al., 2012).

Table 1. Particle Size Distribution (PSD) of materials used for batch experiments

PSD, µm	**Glass Beads (wt.%)**	**Char-LCS (wt.%)**	**Char-SCS (wt.%)**
> 300		16	
300 - 150	16	45	
150 - 105	77	38	
105 - 74	7		31
74 - 53			15
< 53			36
Mean Particle Dia. ($d_{p,avg}$), µm	**132**	**187**	**65**

2.2 Materials used for PCS Testing

Fresh ilmenite was provided by GE Power (formerly ALSTOM Power, Inc.) with a calculated mean particle diameter ($d_{p,avg}$) of 210 µm and size distribution shown in Table 2. To better simulate an OC that has undergone attrition in an actual CLC environment, the 210 µm ilmenite was blended with a finer ilmenite to obtain a new size distribution with a new $d_{p,avg}$ of 170µm. The blended ilmenite (($d_{p,avg}$-170 µm) has a U_{mf} that is approximately 50 percent lower than the fresh ($d_{p,avg}$ = 210 µm) ilmenite. A sample of bed material obtained from GE Power's pilot CLC unit was analyzed to determine the char size distribution. The $d_{p,avg}$ obtained was 108 µm, and the size distribution is shown in Table **2**. Activated carbon was selected as a char substitute and the size distribution was kept the same as for GE Power's sample. However, during testing the $d_{p,avg}$ of the AC varied from 108 µm to 190 µm. This was due to losses of fine particles (less than 105 µm) during testing.

Table 2. PSD of materials used for continuous flow experiments

PSD (µm)	210 Ilmenite, %	170 Ilmenite, %	Char, %
> 300	2	2	9
300 - 150	91	73	25
150 - 105	4	8	21
105 - 74	3	15	17
74 - 53		2	28
Mean Part. Dia., µm	210	170	108

2.3 Analytical Method

To determine the separation efficiency of the units, fractional representative samples of approximately 1 kg were obtained from the recycle stream and clean OC stream by using a riffle splitter. The samples were then combusted at 600°C in enriched air (33% O_2) using a tube furnace. The CO_2 released was measured by a Laser Gas Analyzer from Atmosphere Recovery, Inc. The volume of CO_2 evolved and the ash content of the char were used to determine the char loading of the sample. For runs showing promising char stripping results, a new representative sample was obtained and sieved to four particle sizes: super-300 µm, 300 – 150 µm, 150 – 105 µm and sub-105 µm. For the super-300 µm and sub-105 µm sizes, the amount of solids recovered was too small for analysis in the tube furnace (see Table **2**) and a representative sample was obtained by riffle splitter and analyzed using a Total Organic Carbon Analyzer from Shimadzu.

2.4 LCS Batch Equipment

The batch test unit consisted of a 15 cm internal diameter bed constructed of acrylic with a 45 µm mesh screen supported by an acrylic grid plate. Figure 2 is an image of the set-up. For testing, 4.6 kg of glass beads ($d_{p,avg}$ 132 µm) were mixed with 1 weight percent (wt. %) of char. The bed operating velocity (U_{op} = 0.10 cm/s) used for testing was equal to the minimum fluidization (U_{mf}) of the char. Segregation at this velocity will confirm the theory that low bed velocities for dissimilar solids promotes segregation. Bed flow was provided by a 100 SLPM Sierra mass flow controller. Two test conditions were investigated, the first involved operating the bed as a bubbling bed and the second involved modifying the fluidization of the bed.

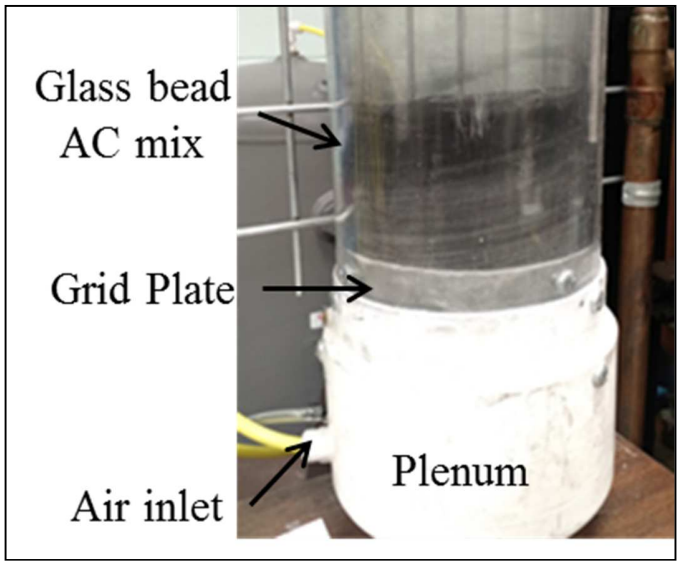

Figure 2. LCS Batch Unit

2.4.1 LCS Separation Principle

The LCS separation principle consists of modifying the fluidization in a bubbling bed to promote the preferential segregation of larger and lighter particles to the top of the bed while minimizing mixing. The LCS relies on the difference in minimum fluidization velocity (U_{mf}) of char and OC. Fluid beds are known for their good mixing characteristics (Kunii and Levenspiel, 1991), however, when dissimilar solids are used, some segregation of the lighter solid to the top of the bed is observed at low bed velocities (Keller, 2012; Rowe and Nienow, 1976). By modifying the fluidization mode, it is possible to promote the segregation of lighter particles to the top of the bed while minimizing overall bed mixing. This principle is tested in the LCS by varying bed operating velocity (U_{op}) in multiples of U_{mf} and changing the bed fluidization mode. During LCS testing, the segregation difficulty, defined here as the difference between the OC and char $d_{p,avg}$, changed. Difficulty is expected to increase as the difference in $d_{p,avg}$ and U_{mf} reduces. Three modes were tested and are summarized in Table 3.

Table 3. LCS Fluidization Modes Tested

Fluidization Mode	Description
A	Bubbling Mode
B	Modified Fluidization
AB	Combination of both

2.5 SCS Batch Equipment

The SCS separation principle relies on differences in terminal velocities between the char and oxygen carrier particles. The equipment was designed as a high velocity vertical cylindrical tube with a countercurrent solids-gas flow pattern; solids fed from the top and gases from the bottom. A 45 µm mesh screen was used as the grid plate and loop seals were used to control solids feed and bed inventory. Air was provided by a compressor and controlled with the 100 SLPM Sierra mass flow controller. The operating velocity for the air was based on the transport velocity of the char particle size tested and ranged from 25 to 60 cm/s. This range covers the recommended velocities for char strippers in literature (Abad et al., 2015). Samples (entrained versus retained) obtained from testing were analyzed using a Total Carbon Analyzer from Shimadzu.

2.6 PCS Continuous Equipment

Two integrated PCS units were constructed – a hot flow unit and cold flow unit. The cold flow unit was designed to test 500 kg/hr of oxygen carrier-carbon mix at room temperatures and different residence times, while, the hot flow system was designed for 50 kg/hr at temperatures up to 800°C.

2.6.1 PCS Hot Flow Unit

Figure 3 is a schematic of the PCS unit.The unit is designed as a once-through system and consists of a feed bed for pre-heating the OC/char mix, a LCS unit with internal dimensions of 15 cm (width), 30 cm (length) and 15 cm (bed height), SCS unit with an internal diameter of 7.6 cm and height of 62 cm, two hoppers for the LCS and SCS and loop seals connecting the different units. The LCS hopper is for collecting the char-rich mix separated from the unit and referred to as the "recycle stream hopper." In an actual CLC system, the recycle stream will be returned to the reducer. The SCS hopper is for the char-lean OC from the LCS unit and is referred to as "clean OC hopper." The material in this hopper is what will go to the oxidizer in a CLC system. Cyclones and fabric filters are used to recover any elutriated particles from all the units. All units are equipped with thermocouples (monitoring and controlling bed temperatures) and pressure transducers (operation of the loop seals and the LCS). Compressed nitrogen (N_2) was used as the fluidizing medium for the feed bed, loop seals and LCS. Compressed carbon dioxide (CO_2) was used for the SCS. Design parameters are summarized in Table 4 and include average operating conditions at which testing was performed.

2.6.2 PCS Cold flow Unit

The cold flow unit is a scale up of the hot flow unit and is built of clear plastic. The cross-sectional area of the LCS is 1.8 times that of the hot flow unit. Design parameters are summarized in Table 4. For the cold flow unit, the maximum bed velocity was 6.2 cm/s due to equipment limitations, so all testing was done at a bed velocity less than or equal to 1 U_{mf}. Testing on the PCS Cold Flow unit focused only on the LCS unit.

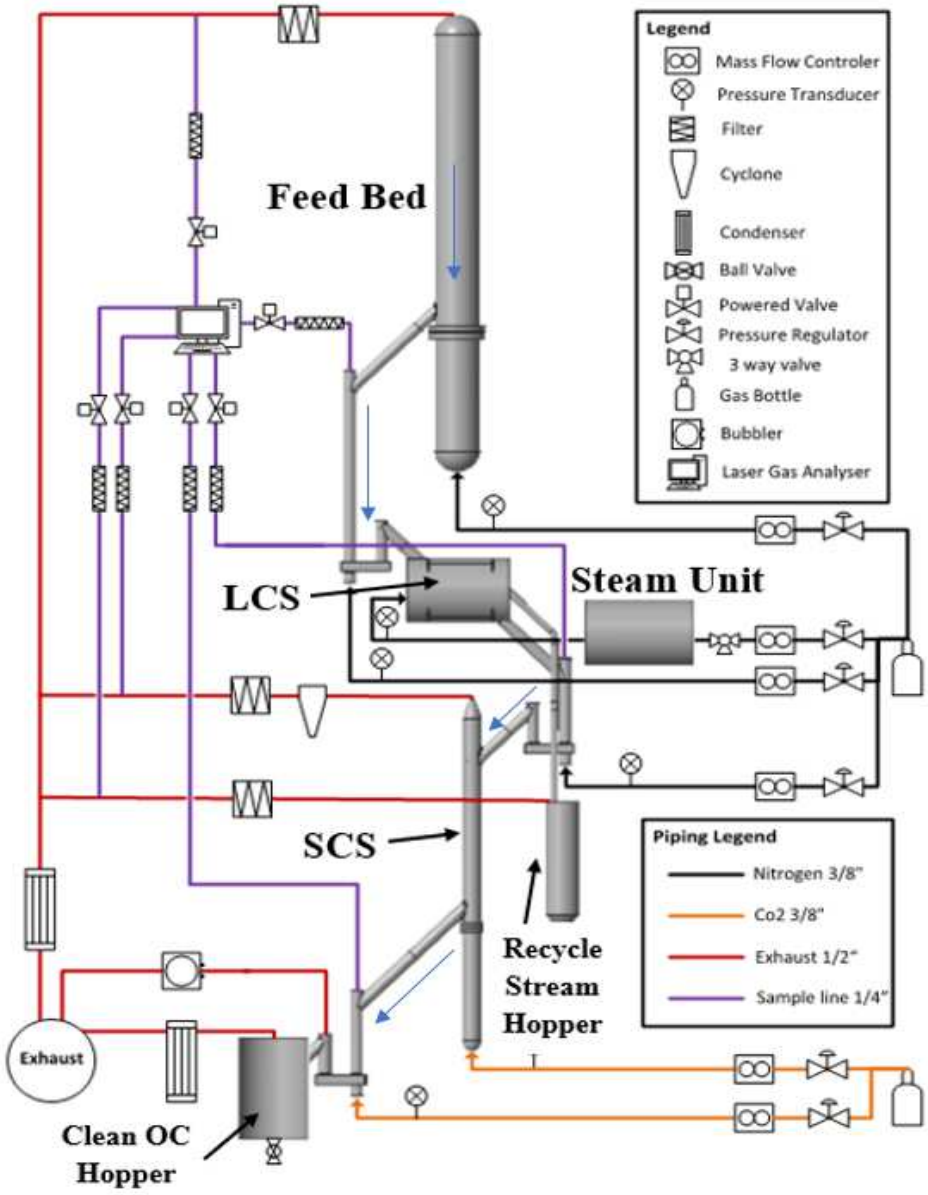

Figure 3. LCS Continuous Flow Unit

Table 4. Operating Conditions of Cold and Hot Flow PCS Units

	COLD FLOW UNIT		HOT FLOW UNIT		
Temperature, °C	21		300	800	
OC Mean Particle Dia., µm	170	210	210	170	210
Solids Feed, kg/hr	250 - 510	380 - 480	31 - 86	74 - 91	53 - 66
Solids Residence Time, min	5 – 23	5 - 8	17 - 47	16 - 20	22 - 28
Bed Velocity, cm/s	2.6	4.6 – 6.2	4.3 – 9.9	3.2	3.1 – 6.2
Min. Fluidization Vel., cm/s	2.6	6.2	4.2	2.2	3.1
Char Content, % OC	0.16 – 0.21	0.63 – 0.73	0.48 – 0.95	0.14	0.13 – 0.21

2.7 PCS Test Methodology

Oxygen carrier (OC) is pre-mixed with the char for a target char loading of 0.5 to 1% and then loaded in the feeder/hopper of the hot/cold unit respectively. For hot flow, the mix is heated to the target temperature under N_2. Once at temperature, gas flow to the LCS and SCS are adjusted to obtain the desired bed velocities, and loop seal 1 (LS1) and 2 (LS2) are turned on to fill the LCS unit and SCS unit respectively. The bed height in the LCS is monitored using three pressure transducers located at heights of 5 cm, 13 cm and 15 cm. The discharge point from the LCS to the recycle stream is at the 15 cm mark. The pressure transducers are also used to determine the solids feed rate of the loop seals by monitoring how rapidly the bed rises and drops. The loop seals are calibrated during every run as loop seal feed rate is very sensitive to varying process temperatures. This sensitivity is due to the design of the loop seal and operation of the unit as a once-through system.

For steady-state operation, LS1 is operated at approximately 20 percent higher feed rate than LS2 so that the overflow in the LCS results in a 20 percent split of recycle stream and clean OC. However, the difference in feed rates between LS1 and LS2 varied from 10 to 30 percent during testing.

Performance metrics for testing is a char separation of 80 percent to the recycle stream and a total recycle stream quantity of 20 percent of the OC feed entering the LCS.

3 RESULTS and DISCUSSION

3.1 Batch LCS Operation

For the batch tests, the char was “sandwiched” between two layers of oxygen carrier surrogate (glass beads) to observe the behavior of the char under the two fluidization conditions tested. Figure 4 is a chronological image showing how the bed changes under regime A (Table 3). The char can be seen making its way to the top of the bed; however, there is an appreciable amount of back mixing that occurs as some of the char also migrates down into the bed. This mixing of material is characteristic of fluid beds. For the second condition, changes to bed fluidization were made with the goal of eliminating or minimizing the back-mixing and improving the char movement to the top of the bed. Figure 5 is an image showing the results. The char is seen migrating to the top of the bed with limited back-mixing. At the end of the test, most of the char can be seen to have migrated to the top of the bed, and a significantly lower quantity of char is observed to be distributed in the vertical direction compared to the standard fluidization mode.

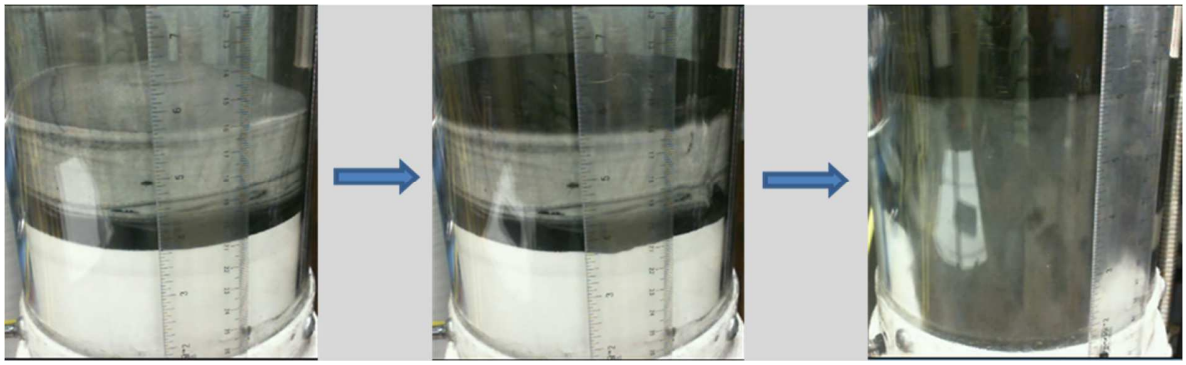

Figure 4. Char segregation during bubbling mode at normal operating conditions

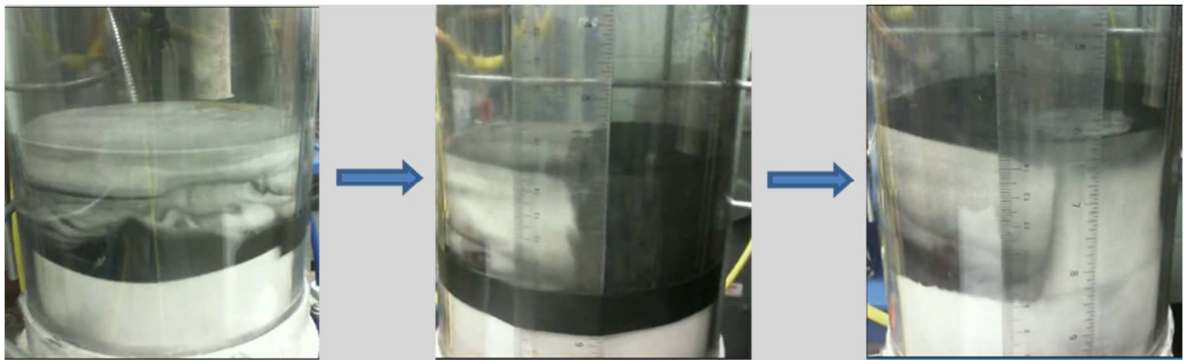

Figure 5. Char segregation at modified bed operating conditions

3.2 Batch SCS Operation

Testing focused on elutriation performance of the SCS as a function of char size distribution. Elutriation versus bed velocity was determined and is shown in Figure 6.

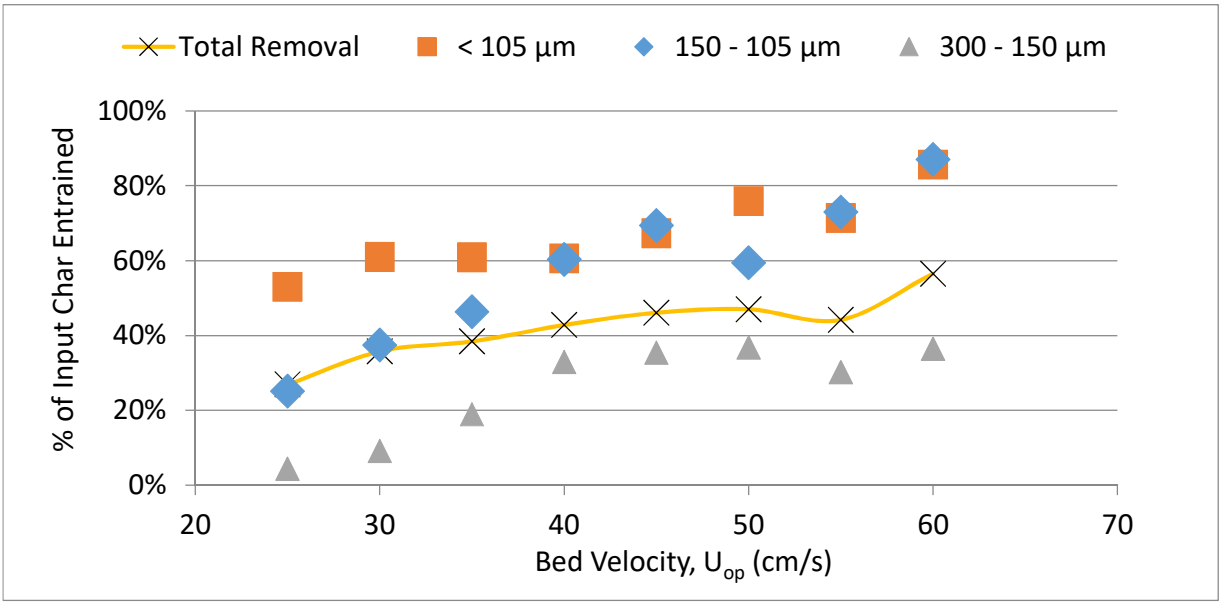

Figure 6. Entrainment efficiency of SCS unit

Separation for this unit is governed by particle terminal velocities and their separation efficiencies in the SCS (Kramp et al., 2012). Figure 6 shows that higher flows lead to higher elutriation of char that is finer than 150 µm. However, for char coarser than 150 µm, the elutriation rate plateaus. These results show some agreement with literature. Kramp et al. (Kramp et al., 2012) showed that for a coal with a top particle size of 200 µm and density of 750 kg/m^3 the terminal velocity is greater than 60 cm/s. So to improve removal of the 300 – 150 µm carbon fraction, velocities greater than 60 cm/s are needed. Sun et al. (Sun et al., 2015) observed similar removals (45 percent at 40 cm/s bed operating velocity) to our work when using plastic beads with a density of 1226 kg/m^3 and a median particle diameter of 208 µm. Abad et al. (Abad et al., 2015) say that for a coal size of 100 µm and density of 1000 kg/m^3 a velocity of 35 cm/s in the stripper gave a stripper efficiency of at least 70 percent, which is higher than the 60 percent for the SCS (char finer than 105 µm). This difference is most likely due to a better separation efficiency in the unit used by Abad compared to the SCS unit. An operating velocity (U_{op}) of 40 cm/s was selected as optimal for the char size distribution tested. This corresponds to a 43 percent total removal.

3.3 PCS Continuous Test

3.3.1 Cold Flow Test

Cold flow testing focused on performance of the LCS which presents a novel approach to segregating char.

3.3.1.1 210 µm ($d_{p\ avg}$) Ilmenite

The three fluidization modes listed in Table 3 were tested using the cold flow LCS unit to identify the most promising fluidization regime for additional testing. Specific bed operating conditions are summarized in Table 5 and the results obtained are summarized in Figure 7. The AB regime gave the best performance with 64 percent char removal in a 16 weight percent recycle stream. Corresponding performances were 63/19 percent and 61/30 percent for char removal/recycle stream quantity for regimes B and A respectively. Char removals for all three tests were similar, however, a higher recycle stream was required for Regime A (test 1) . Regime AB (test 3) had the lowest required recycle stream quantity and was therefore selected for additional testing, with a focus on attaining the 80 percent char removal target.

Table 5. Operating conditions for cold flow testing of 210 µm Ilmenite at different fluidization regimes

Test	1	2	3
Fluidization Regime	A, 1 U_{mf}	B, 0.75 U_{mf}	AB 1 U_{mf}
Solids Feed, kg/hr	405	389	478
Solid Residence Time, min	14	15	12
Mean Char Size, µm	146	135	na

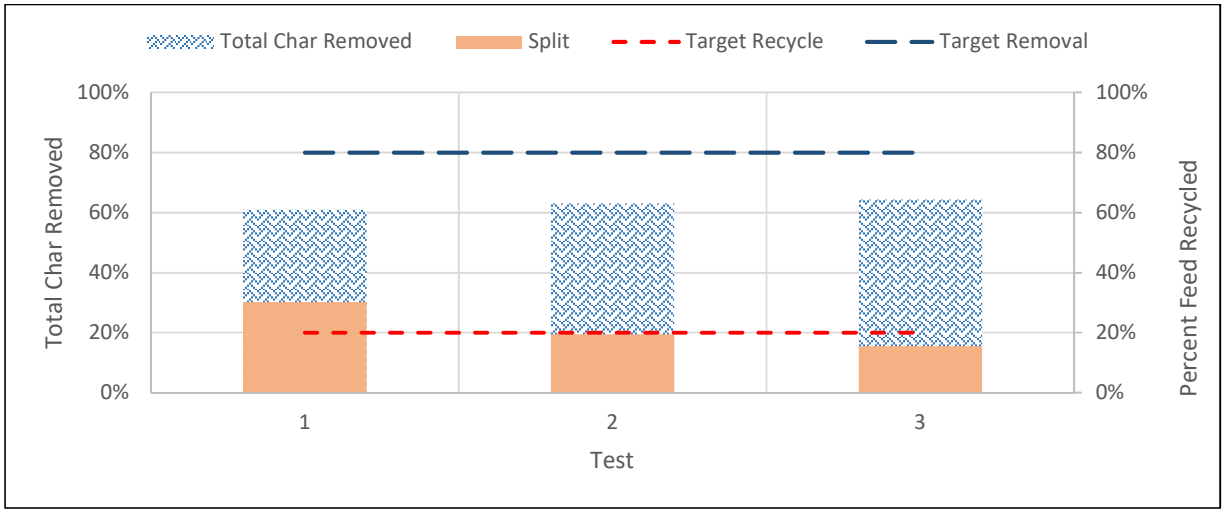

Figure 7. Cold flow LCS test results of 210 µm Ilmenite for 3 tests. Fluidization modes for tests in Table 5.

One key observation during operation of the cold flow system was the pooling of char on top of the bed. The bed design (single exit point at top) resulted in char accumulation dead zones, which could explain the improved performance at higher splits – a larger fraction of the bed surface is removed as a result of the higher feed rate at the bed surface.

3.3.1.2 170 µm ($d_{p\ avg}$) Ilmenite

Testing with the 170 µm ilmenite was conducted only for the AB fluidization regime. Seven tests investigated the effect of bed height and feed rate/residence time on performance. Figure 8 and Table 6 summarize the results of the tests and the operation conditions. The segregation difficulty for these tests was higher ($d_{p,avg}$ of OC = 170 µm and $d_{p,avg}$ of char = 110 to 136 µm) as the 170 µm Ilmenite has a 50 percent lower U_{mf} (Table 4) than the larger oxygen carrier tested earlier.

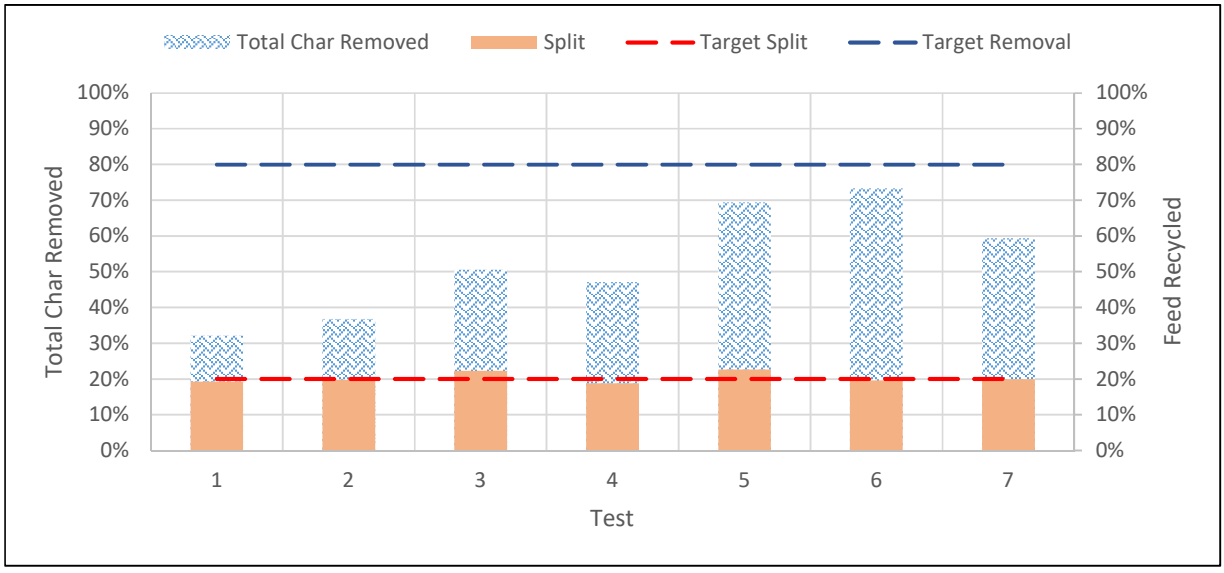

Figure 8. Cold flow LCS tests of 170 µm Ilmenite at different bed heights and solid feed rates. Bed velocity during all tests 1 U_{mf} equivalent with AB fluidization regime

Table 6. Operating conditions for cold flow testing of 170 µm Ilmenite at 1 Umf and AB fluidization regime

Test	1	2	3	4	5	6	7
Solids Feed, kg/hr	483	463	246	514	254	243	452
Residence Time, min	5	6	10	5	20	21	23
Bed Height, cm	15	15	15	15	31	31	62
Mean Char Size, µm	128	na	136	123	na	110	131

Effect of Bed Height and Residence Time: Residence time is defined as the solids inventory of the unit divided by the solids feed rate. This assumes solids residence is similar to a plug flow reactor (PFR) which is not considered an accurate representation of the unit as addressed in section 3.3.2.1. The residence time as defined is thus adopted to facilitate comparison between operating conditions. By doubling the bed height and maintaining the feed rate (doubling residence time), char removal increased significantly by at least 20% (test 1/2 vs 7, test 3 vs 5/6). Doubling the feedrate, while maintaining bed height (halved residence time), resulted in a 3 to 18% drop in char removal (test 3 vs 1/2/4). Doubling the feedrate and doubling the bed height to keep residence time the same (test 5/6 vs 7) resulted in a slight drop in char removal performance. These results suggest increasing residence time and bed height improved performance. Taller bed heights are desired, as they reduce the square foot print of the facility. Longer residence times imply larger equipment volume. At the low bed velocities/fluidization at which the LCS is operated, poor solids mixing of the bed is expected, and channelling/bypassing of the bed is likely. It was not possible to confirm the occurence of channeling in this system due to the high feed rates and design limitations, but it is important to confirm its occurence as it would provide a better picture on the effect of residence time during scale up.

Segregation Efficiency of Char Particle Size: To better understand the effect on particle size, char compositions of the recycle stream and clean OC stream were analyzed for different size fractions. Figure 9 summarizes the char removal efficiencies in different particle size bins. Runs 2 and 5 were not included as a size distribution analysis of the samples was not available. For both runs 6 and 7, a relative increase in performance for the coarse char (greater than 150 µm) is observed suggesting a positive effect of increased bed height or residence time on removal of coarser particles. Fine char (74 to 150 µm size bin) showed low removal efficiency which could be due to the lower bed velocity (U_{mf} = 2.6 cm/s) for the 170 µm Ilmenite. Overall, test 6 had the best results, and comparison of data for the different sizes (Figure 9) showed the best performance for the coarse char particles.

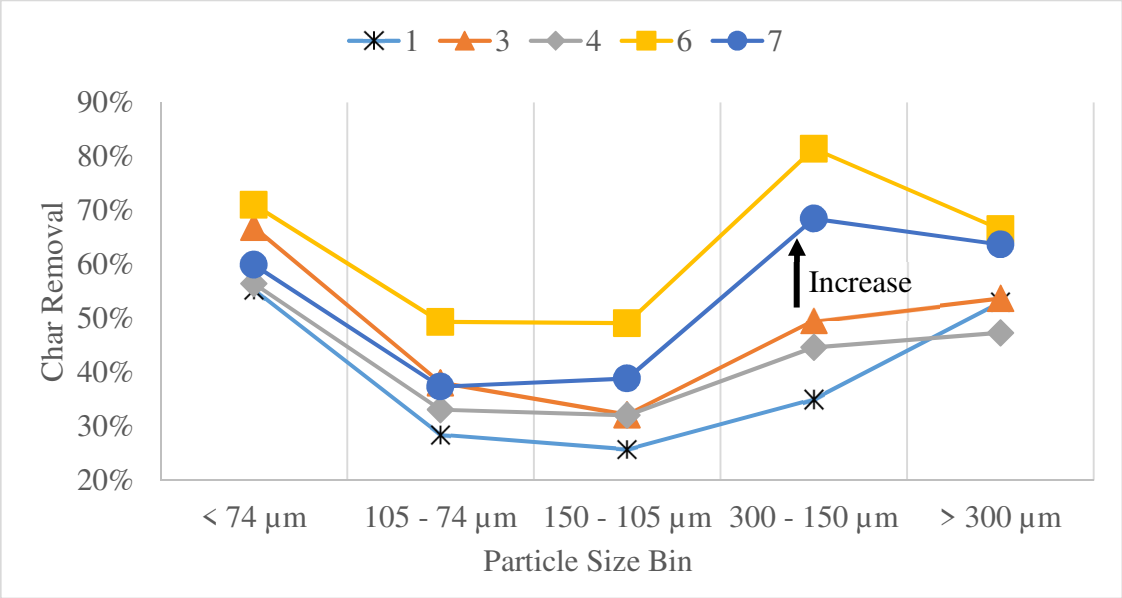

Figure 9. Cold flow removal efficiency of char for different size bins

In summary, the cold flow results suggest that two possible factors influence char segregation performance in the LCS: 1) a sufficient solids residence time is needed for the char to effectively segregate to the top of the bed, and 2) a taller bed makes it less likely for feed material to bypass the bed, resulting in improved char separation.

3.3.2 Hot Flow PCS Test

3.3.2.1 Testing at 300°C

Preliminary hot flow testing to establish operating parameters and run conditions for the hot flow system was performed at 300°C. This temperature was selected to eliminate potential issues from the presence of moisture, but also to understand the effect of temperature on the operation of loop seals while minimizing oxidation of the char by the OC. Table 7 and Figure 10 show the results for the PCS unit along with the corresponding test conditions. Testing was with the 210 µm Ilmenite and focused on fluidization regimes A and AB.

To minimize the effect of heat losses in the loop seals, the setpoint for pre-heating the solids was 500°C resulting in a feed stream at a slightly higher temperature than the solids in the LCS. This made it possible to use thermocouples inserted in different locations in the LCS unit to provide information on the extent of solids mixing. During operation, the temperature reading on several thermocouples in the LCS unit showed little to no change except for locations next to the char exit and OC exit (see Figure 1). This implies very poor mixing was occuring in the bed and the actual residence time of the solids was shorter than the calculated value.

Effect of Temperature: To verify if temperature had an effect on performance, Test 2 at 300°C (Table 7) was compared to Test 3 of the cold flow system (Table 5). The residence times were 17 and 12 minutes respectively, the fluidization regime was the same and bed operating velocity were

both equivalent to 1 U_{mf}. Test 2 (300°C) saw a similar AC removal of 66 percent with Test 3 (cold flow) of 64 percent. Doubling the operating temperature from room conditions (≈ 293 K) to 300°C (573 K) did not have a significant effect on performance.

Comparison of Regime A and AB: Comparing test 2 (Regime AB) to test 1 (Regime A), the feed rate was doubled, bed velocity halved and the material split kept the same (Table 7). Results showed similar char removals (Figure 9). The higher throughput of test 2 reduced the solids residence time, thus translating to a smaller equipment volume for this case. It was also operated at half the bed velocity of test 1 – a lower bed velocity implies a smaller pressure drop and ultimately lower operating costs. Comparing test 4 (Regime AB) to test 1 (Regime A), the residence times were similar but the recycle stream for test 4 was 32 percent with a high AC removal of 83 percent. Regime A, be it in the cold flow tests (Table 5, test 1) or the 300°C tests (Table 7, test 1), did not demonstrate removal efficiencies higher than 65%, with both a high recycle stream (30%, cold flow) and high solids residence time (36 min, 300°C). The above data imply that fluidization in the AB regime can achieve better char removal targets at lower operating velocity (costs) than regime A.

Table 7. Operating conditions during 300°C shakedown of hot flow PCS Unit

Test Condition	1	2	3	4
Fluidization Regime	A, 2 U_{mf}	AB, 1 U_{mf}	AB 2 U_{mf}	AB, 2 U_{mf}
Solids Feed, kg/hr	40	86	72	42
Residence Time, min	36	17	20	34
Mean Char Size, µm	165	188	175	na

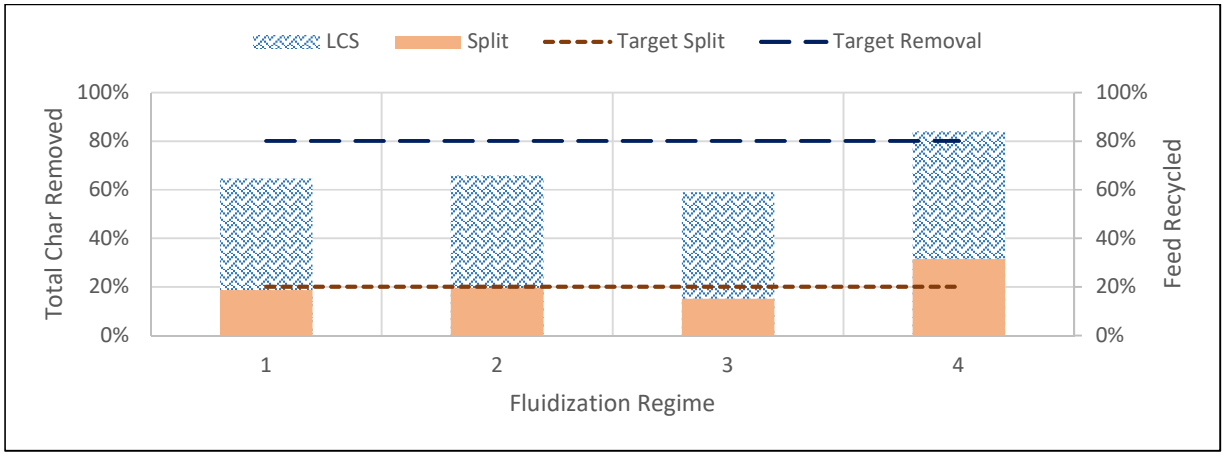

Figure 10. Hot flow (300°C) test results at 2 fluidization modes – A and AB

Segregation Efficiency of char: The segregation difficulty for the 300°C tests was higher than that for the cold flow tests (Char $d_{p,avg}$ was 165 - 188 µm for 300°C tests vs 135 – 146 µm for cold

flow tests). Comparing results at hot flow (Figure 10) and cold flow (Figure 7), the larger $d_{p,avg}$ of the char did not appear to adversely affect the performance of the PCS system.

3.3.2.2 Testing at 800°C

Two OC particle size distributions were investigated at 800°C with $d_{p,avg}$ of 210 and 170 µm respectively. Actual test conditions during 800°C tests are summarized in Table 8. The temperature of the LCS and SCS during testing was determined by averaging the inlet and outlet temperatures of the char-oxygen carrier mix. During temperature ramp up, some char conversion to CO and CO_2 was observed in the feed bed so the mean particle diameter of the char was determined at the end of every test.

Table 8. Operating conditions of hot flow 800°C testing

Test	1	2	3	4	5	6
Fluidization	AB				A	AB
Particle Size, µm	210				170	
Bed Velocity ÷ U_{mf}	2	2	1	1.5	1.5	1.5
Solids Feed, kg/hr	57	60	66	53	74	90
LCS Residence Time, min	25	24	22	28	20	16
Average LCS Temp., °C	726	703	702	747	683	705
SCS Bed Velocity, cm/s	40	44	38	42	38	42
SCS Performance, %	1%	2.4%	2.1%	2.0%	1.5%	2.1%
Average SCS Temp., °C	587	675	561	648	546	649
Mean Char Size, µm	131	113	122	110	116	117

Performance of PCS: Figure 11 is a summary of performance results of the PCS system. For test 1, 2 and 3, the removal target of 80 percent was met with 27%/26%/23% split between the recycle/feed respectively. For runs 4, 5 and 6, removal was 74%/74%/78% with splits of 16%/13%/15% respectively. Residence times for tests 1 to 3 were similar (22 - 25 min.) with operating bed velocities between 1 - 2 U_{mf}, suggesting that the recycle stream quantity is the most important factor for separation. Overall separation efficiency improved when compared to cold flow and 300°C tests. Analysis of the char size distribution showed that this was due to a higher performance of the system in terms of separating fine char particles (see discussion below).

Effect of OC Particle Size: Test 5 and 6 for 170 µm Ilmenite are meant to simulate an attrited oxygen carrier during CLC. Comparing test 4 to 5/6 (identical bed velocities), we observe similar performance even though feed rates are higher for 5 and 6. The solids throughput for test 4 and 6 increased 1.7 times and char removal saw a 4 percent increase for test 6 over test 4. This suggests that OC attrition did not negatively impact performance for the range of conditions tested. Also,

during testing of the 170 µm Ilmenite, the recycle stream showed a slight enrichment in its fines loading, confirming the separation principle of the LCS that differences in U_{mf} are the driving force for segregation.

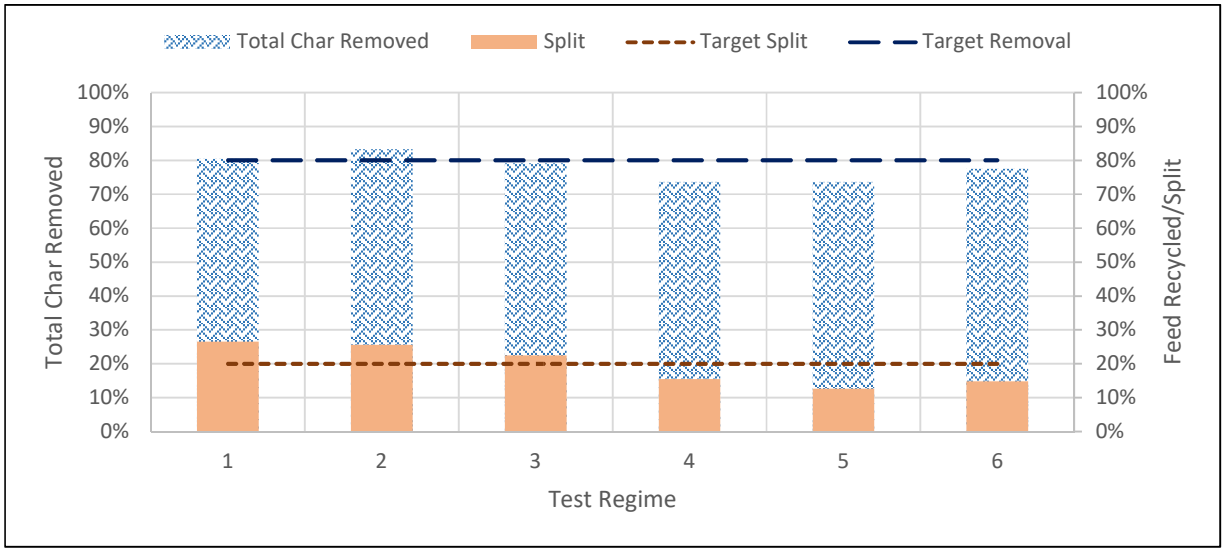

Figure 11. Hot flow test results at 800°C with 210 µm Ilmenite (1 - 4) and 170 µm Ilmenite (5 – 6)

Performance of SCS: Table 8 shows the removal performance for the SCS while operating at an average bed velocity of 41 cm/s. Less than 2.5 percent of the total char removal for the PCS system was from the SCS. The finer the particle, the lower its transport velocity. Even though the large char separator is operated at low velocities, the minimum fluidization velocity of the denser and large oxygen carrier particles can overlap with the transport velocity of fine char particles. Also, during fluidization, the bed is characterized by regions of high velocity which facilitates transport of fine char particles to the top of the LCS bed. All these factors make the LCS effective in segregating small char particles and thus effective in removing both fine and coarser char.

Segregation Efficiency as a function of Char Particle Size: Figure 12 shows the removal efficiency for the different size bins of the char. As discussed earlier, the high removal efficiencies of 67 to 99 percent observed for the fine sizes occured mainly in the LCS. Cold flow testing which focused only on the LCS had smaller removal percentages for the same size bin (28% to 71%, (Figure 9)). The difference is attributed to moisture content of the OC used for the cold flow which likely caused the fine AC to "stick" on to the oxygen carrier particles. For the 300 to 150 µm size bin, the removal data showed good agreement for all runs, with separation averaging 60%. For particles larger than 300 microns, removal efficiency was quite variable.

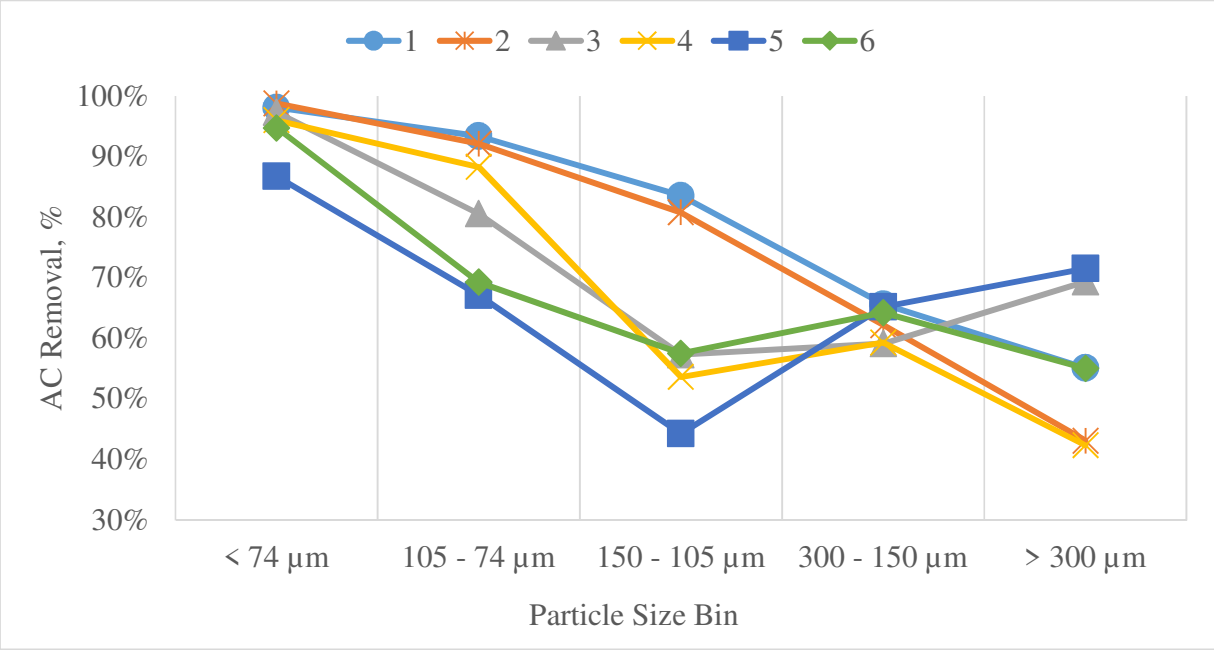

Figure 12. Hot flow 800°C PCS Removal efficiency of AC by size bins

4 CONCLUSIONS AND FUTURE WORK

Development work on a Particle Char Separator (PCS) system for chemical looping combustion is presented with performance results for ambient and higher temperature operation and for varying material feed rates. The PCS comprises a large char separator (LCS) unit which focuses on removal of char particles greater than 150 µm, and a small char separator unit (SCS), which targets removal of smaller-sized particles.

Proof-of-Concept testing confirmed that low bed velocities, close to minimum fluidization, can be an effective tool for separating char from oxygen carrier material, if an appropriate fluidization mode is used. A modified fluidization mode consistently showed better performance than standard fluidization with the ratio of bed velocity to minimum fluidization equal to or less than 2. This is an important finding, as a lower bed velocity would imply lower operating cost when at full scale.

PCS testing of the hot flow system demonstrated that removal of 80 percent of char particles pre-mixed with oxygen carriers was possible with only a 20 percent recycle of the feed solids. Char particles with sizes that are similar or large size than the oxygen carrier (greater than 150 µm) were removed with efficiencies of 42 to 81 percent, while smaller char particles (less than 150 µm) were removed with higher efficiencies (44 to 99 percent). This range in performance suggests that tailoring of oxygen carrier and fuel particle sizes could be used to maximize separation.

Factors that seem to influence separation performance the most were 1) the fraction of solids recycled during modified fluidization – higher fractions consistently resulted in higher removal performance. This was due to the mitigated impact of dead zones on the bed surface. 2) The

average residence time of solids and 3) the bed height. Increasing both residence time and bed height resulted in better results, however, more work is required to fully understand their impacts. Future work will focus on determining the true residence time of the solids in the PCS system and understanding its effect on char conversion.

Finally, all the testing was conducted using a once-through design. Future work will look at incorporating the large char separator with a 10 kW chemical looping combustion test unit to evaluate its performance under CLC and circulating conditions. Improvements to system design such as a better feed discharge location, is expected to further improve the char removal efficiency at similar oxygen carrier recycle ratios.

5 ACKNOWLEDGEMENTS

This material is based upon work supported by *The United States Department of Energy* under Award Number DE-SC0013832.

6 References

[1] Abad, A., Adànez, J., Gayán, P., de Diego, L.F., García-Labiano, F. and Sprachmann, G. (2015) 'Conceptual design of a 100 MWth CLC unit for solid fuel combustion', *Applied Energy*, pp. 462-474.

[2] Abad, A., Adànez-Rubio, I., Gayán, P., García-Labiano, F., de Diego, L.F. and Adánez, J. (2012) 'Demonstration of chemical-looping with oxygen uncoupling (CLOU) process in a 1.5 kWth continuously operating unit using a Cu-based oxygen-carrier', *International Journal of Greenhouse Gas Control*, vol. 6, pp. 189-200.

[3] Abad, A.A.J., Cuadrat, A., Garcìa-Labiano, F., Gayán, P. and de Diego, L.F. (2011) 'Kinetics of Redox Reactions of Ilmenite for Chemical-Looping Combustion', *Chemical Engineering Science*, vol. 66, pp. 689-702.

[4] Abad, A., Pérez-Vega, R., de Diego, L.F., García-Labiano, F. and Gayán, P.A.J. (2015) 'Design and operation of a 50 kWth Chemical Looping Combustion (CLC) Unit for Solid Fuels', *Applied Energy*, vol. 157, pp. 295-303.

[5] Adànez, J., Abad, A., Mendiara, T., Gayán, P., de Diego, L.F. and Garçia-Labiano, F. (2018) 'Chemical looping combustion of solid fuels', *Progress in Energy and Combustion Science*, vol. 65, pp. 6-66.

[6] Azis, M.M., Leion, H., JErndal, E., Steenari, B.-M., Mattison, T. and Lyngfelt, A. (2013) 'The Effect of Bituminous and Lignite Ash on the Performance of Ilmenite as Oxygen Carrier in Chemical-Looping Combustion', *Chemical Engineering Technology*, vol. 36, no. 9, pp. 1460-1468.

[7] Bayham, S., McGiveron, O., Tong, A., Chung, E., Kathe, M., Wang, D., Zeng, L. and Fan, L.-S. (2015) 'Parametric and dynamic studies on an iron-based 25-kWth coal direct chemical looping unit using sub-bituminous coal', *Applied Energy*, vol. 145, May, pp. 354-363.

[8] Cuadrat, A., Abad, A., Adànez, J., de Diego, L.F., García-Labiano, F. and Gayán, P. (2012) 'Behavior of ilmenite as oxygen carrier in chemical-looping combustion', vol. 94, no. 1, pp. 101-112.

[9] Gu, H., Shen, L., Zhong, Z., Niu, X., Ge, H., Zhou, Y. and Xiao, S. (2014) 'Potassium-Modified Iron Ore as Oxygen Carrier for Coal Chemical Looping Combustion: Continuous Test in 1 kW Reactor', *Industrial & Engineering Chemistry Research*, vol. 53, no. 33, pp. 13006-13015.

[10] Johannson, J. (2016) *Oxygen polishing of chemical looping combustion flue gases (Master's Thesis)*, Sweden: Chalmers University of Technology, Available: http://publications.lib.chalmers.se/records/fulltext/244942/244942.pdf [11 May 2018].

[11] Keairns, D., Kuehn, N., Newby, R. and Shah, V. (2014) *Guidance for NETL's Oxycombustion R&D Program: Chemical Looping Combustion Reference Plant Designs and Sensitivity Studies*, National Energy Technology Laboratory.

[12] Keller, N.K.G. (2012) *Mixing and Segregation in 3D multi-component, two-phase fluidized beds. PhD Dissertation*, Ames: Iowa State University.

[13] Kim, H.R., Wang, D., Zeng, L., Bayham, S., Tong, A., Chung, E., Kathe, M.V., Luo, S., McGiveron, O., Wang, A., Sun, Z., Chen, D. and Fan, L.-S. (2013) 'Coal direct chemical looping combustion process: Design and operation of a 25-kWth sub-pilot unit', *Fuel*, vol. 108, pp. 370-384.

[14] Kramp, M., Thon, A., Hartge, E.-U., Heinrich, S. and Werther, J. (2012) 'Carbon Stripping - A Critical Process Step in Chemical Looping Combustion of Solid Fuels', *Chemical Engineering and Technology*, vol. 35, no. 3, pp. 497-507.

[15] Kunii, D. and Levenspiel, O. (1991) *Fluidization Engineering*, Boston: Butterworth-Heinemann.

[16] Linderholm, C. and Lyngfelt, A. (2017) 'Chemical-Looping Combustion of Solid Fuels - Status and recent progress', *Energy Procedia*, vol. 114, pp. 371-386.

[17] Markström, P., Linderholm, C. and Lyngfelt, A. (2013) 'Chemical-looping combustion of solid fuels - Design and operation of a 100 kW unit with bituminous coal', *International Journal of Greenhouse Gas Control*, vol. 15, pp. 150-162.

[18] Mendiara, T., Pérez-Astray, A., Izquierdo, M.T., Abad, A., de Diego, L.F., Garcìa-Labiano, F., Gayàn, P. and Adànez, J. (2018) 'Chemical Looping Combustion of different types of biomass in a 0.5 kWth unit', *Fuel*, vol. 211, pp. 868-875.

[19] Recio, A., Chen Liew, S., Lu, D., Rahman, R., Macchi, A. and Hill, J.M. (2016) 'The Effects of Thermal Treatment and Steam Addition on Integrated CuO/CaO Chemical Looping Combustion for CO2 Capture', vol. 4, no. 11.

[20] Rowe, P.N. and Nienow, A.W. (1976) 'Particle mixing and segregation in gas fluidised beds. A review', vol. 15, pp. 141-147.

[21] Sahir, A.H. (2013) *Process modeling aspects of Chemical-Looping with Oxygen Uncoupled and Chemical-Looping Combustion for solid fuels*, Department of Chemical Engineering, University of Utah.

[22] Ströhle, J., Orth, M. and Epple, B. (2015) 'Chemical looping combustion of hard coal in a 1 MWth pilot plant using ilmenite as oxygen carrier', *Applied Energy*, pp. 288-294.

[23] Sun, H., Cheng, M., Chen, D., Xu, L., Li, Z. and Cai, N. (2015) 'Experimental Study of a Carbon Stripper in Solid Fuel Chemical Looping Combustion', *Industrial & Engineering Chemistry Research*, vol. 54, no. 35, pp. 8743-8753.

516 [24] Sun, H., Cheng, M., Li, Z. and Cai, N. (2016) 'Riser-Based Carbon stripper for Coal-fueled
517 Chemical Looping Combustion', *Industrial & Engineering Chemistry Research*, vol. 55, pp.
518 2381-2390.

519 [25] Thon, A., Kramp, M., Hartge, E.-U., Heinrich, S. and Werther, J. (2014) 'Operational
520 experience with a system of coupled fluidized beds for chemical looping combustion of solid
521 fuels using ilmenite as oxygen carrier', *Applied Energy*, vol. 118, April, pp. 309-317.

522 [26] Tian, X., Zhao, H., Wang, K., Ma, J. and Zheng, C. (2015) 'Performance of cement decorated
523 copper ore as oxygen carrier in chemical-looping with oxygen uncoupling', *International*
524 *Journal of Greenhouse Gas Control*, vol. 41, October, pp. 210-218.

525 [27] Tong, A., Bayham, S., Kathe, M.V., Zeng, L., Luo, S. and Fan, L.-S. (2014) 'Iron-based
526 syngas chemical looping process and coal-direct chemical looping process development at
527 Ohio State University', *Applied Energy*, vol. 113, pp. 1836-1845.

528 [28] van der Watt, J.G., Laudal, D., Feilen, H. and Mann, M. (2017) 'Attrition and Reactivity
529 Analysis of Oxygen Carrier Materials under High Temperature Conditions', Pittsburgh Coal
530 Conference Proceedings, Pittsburgh.

531 [29] Van Der Watt, J., Laudal, D., Krishnamoorthy, G., Feilen, H., Mann, M., Shallbetter, R.,
532 Srinivasachar, S. and Nelson, T. (2017) 'Development of a Spouted Bed Reactor for
533 Chemical Looping Combustion', Clearwater Conference, Tampa.

534 [30] Viches, T.B., Lind, F., Rydén, M. and Thunman, H. (2017) 'Experience of more than 1000 h
535 of operation with oxygen carriers and solid biomass at large scale', *Applied Energy*, vol. 190,
536 March, pp. 1174-1183.

537 [31] Zeng, L., Kathe, M.V., Chung, E.Y. and Fan, L.-S. (2012) 'Some remarks on direct solid fuel
538 combustion using chemical looping processes', *Current Opinion in Chemical Engineering*,
539 vol. 1, no. 3, pp. 290-295.

540